Jestr

Journal of Engineering Science and Technology Review 16 (5) (2023) 59 - 68

Research Article

JOURNAL OF
Engineering Science and Technology Review

www.jestr.org

Higher Order Shear Deformation Theory for Functionally Graded Porous Beam - Numerical Free Vibrational Analysis

N. K. Geetha[1], G. Chandra Mohana Reddy[2] and P. Bridjesh[2,*]

[1]*Department of Mathematics, Dayananda Sagar College of Engineering, Bengaluru, 560078, India*
[2]*Department of Mechanical Engineering, MLR Institute of Technology, Hyderabad, 500043, India*

Received 30 January 2023; Accepted 16 October 2023

Abstract

This study applies a third order shear deformation theory in order to present free vibration behaviour of two directional functionally graded porous beams (2D-FGPB) at several combinations of boundary conditions. These boundary conditions include being simply supported, clamped- clamped, and clamped- free. In both directions, beam's properties exhibit exponentially changing patterns. Hamilton's principle is utilised so that the free vibration response may be analysed. These equations of motion are derived in order to accomplish this. Polynomial forms are used to express axial, transverse, and rotational deflections of the cross sections. These forms also include auxiliary functions which are utilised to meet the desired boundary conditions. Using the published results from earlier studies, verification and convergence studies are carried out. The gradient indices have a significant impact on the dimensionless natural frequency (λ) of the 2D-FGPB. For SS beam, at px = 1.0, the values of λ are 2.365, 2.340, and 2.299 for pz = 0.1, 0.6, and 1.0, respectively. Likewise for CC beam, at px = 1.0, the values of λ are 5.158, 5.131, and 5.082 for pz = 0.1, 0.6, and 1.0, respectively and for CF beam, at px = 1.0, the values of λ are 0.674, 0.668, and 0.658 for pz = 0.1, 0.6, and 1.0, respectively. The findings of numerous investigations are presented here in order to facilitate an understanding on vibrations in 2D-FGPB of the implications of varying gradient indices, aspect ratios, and boundary conditions.

Keywords: Functionally graded porous beam; third order shear deformation theory; Lagrange's equations; Hamilton Principle; Free vibration.

1. Introduction

Amazing developments in technology in recent years have encouraged researchers to create materials with enhanced qualities. Functionally graded materials (FGMs) are a family of materials that have continuously varying distributions between two or more constituent phases [1]. The majority of current research on FGMs assumed that the material characteristics fluctuated smoothly only in one direction. Due to the uniform composition distribution of the body's exterior and inner surfaces, conventional FGM may not be as helpful in solving design issues [3]. Additionally, by choosing appropriate distinct parameters of power law distribution, the design of such a material profile could be more efficient. A 2D generalised power law is suggested for modelling material qualities in two directions in order to achieve this. The volume fraction is a common variable in engineering studies of FGMs. Volume fractions may vary solely in terms of the structure's thickness or in another direction. Young's modulus, thermal conductivity, Poisson's ratio, thermal expansion coefficient, shear modulus, and material density are a few examples of mechanical [5] and thermal parameters [6] that vary smoothly and continuously in FGMs' preferred orientations.

Structural evaluation, damage detection, and location have always been key topics. Depending on the severity of the damage, a structure's flexibility will often increase locally. This alters the natural vibrational frequencies and modifies the natural mode shapes, effects that have been used to evaluate the degeneration with varying degrees of success. Material properties of functionally graded beams (FGBs) were continuously varied in thickness, which is also consistent with power law. Nguyen *et al.* [7] developed two different formulations, the bending rotation as well as shear rotation as unknown functions. The frequency equations were derived from Lagrange's equations, while the beam's boundary conditions were met. In order to account for bending as well as the free vibration of FGBs, multiple Higher Order Shear Deformation Beam Theories (HSDT) [8, 9] were devised. For the free vibration evaluations in 2D- FGBs having exponentially variable material parameters, a symplectic elasticity solution was provided in [10, 11].

Researchers' interest in Functionally Graded Porous Materials (FGPMs) has lately increased [12]. FGPMs, where the mechanical properties change constantly along the structure. These are compounds that gradually change in porosity across their volume. A gradual change in porosity can be used to provide desirable properties. Using analytical solutions and Euler-Bernoulli theory, Mojahedin *et al*. [13], estimation of natural vibration in functionally graded (FG) thin beam with pores was made. Babaei *et al.* [14] implemented finite element approach to examine buckling, static, and dynamic evaluations of a FG porous thick beam in accordance with HSDT. In another analysis, using beam theories and Navier's solution, Hung *et al.* [15] explored the static behaviour of FGB with a fluid-infiltrating porous core. Gharibi *et al.* [16] implemented Frobenius series approach to compare the stresses in FG rotating thick cylinders to the finite element findings under plane stress and plane strain conditions. Free vibration and stress analysis were executed

*E-mail address: meetbridjesh@gmail.com
ISSN: 1791-2377
doi:10.25103/jestr.165.08

on FGMs using the Ritz method [17], and based on HSDT [18], a four-node quadrilateral plate was proposed to assess static bending as well as vibrational analysis of the FG plates. By incorporating a quadratic shear shape function into terms of higher order and eliminating shear result, transverse shear forces on two sides were avoided. Using a unified model, Karami *et al.* [19] examined the resonance behaviour of nanoplates adapting nonlocal bi-Helmholz strain gradient theory. Using nonlocal elasticity theory, Zarezadeh *et al.* [20] examined the effect of size on FG nano-rods under a magnetic field. To study nonlinear bending, and vibration analysis, numerous studies on bidirectional FGBs, Euler Bernoulli [21], Timoshenko beam theory [22], third order shear deformation theory by Karmanli [23], and the finite element method [24]. Using a quasi-three dimensional shear deformation theory, Zenkour [25] analysed bending reactions of rectangular plates using a new quasi-3D refined theory. Kaddari *et al.* [26] provided a statics along with free vibration study of FG porous plates which are resting on an elastic foundations to assess the effect of porosity.

From the current literature, it could be inferred that classical beam theory disregards shear deformation and offers only relevant solutions to thin beams. Deficiency in Timoshenko beam theory is that it does not accurately predict the behaviour of beams with non-uniform loads or loads applied at an angle to the beam axis. Also, it is only applicable to beams with small deflections, and may not accurately predict the behaviour of beams with large deflections or large deformations. Above all, it does not take into account the effect of rotary inertia, which can be important for beams subjected to high levels of acceleration or impact loads. The quasi-3D theories that incorporate shear deformation as well as stretching in thickness may be mathematically prohibitive in case of complicated geometries [27]. A study on vibrations occurring in FG beams with porosity employing a refined beam theory is needed. In this study, the beam is modelled that is according to HSDT which takes into consideration the influence of porosity with a unique shear shape function along the thickness of the beam. According to current theory, the behaviour of 2D- FGPBs does not need to be adjusted based on the material and shape of the beam or the constraints on its ends.

This article focuses on vibrational analysis of 2D-FGPB when subjected to different types of constraints along with the distribution of the material's attributes follows a power law. Adapting Hamilton's principle and three specific boundary conditions such as simply supported, clamped - clamped, and clamped - free, this article develops a special approach for ensuring that there is no shear stress felt on either the top or bottom surfaces of the beam.

2. Formulation and Mathematics

2.1 Formulation of porous FG beam

The coordinate system for the beam used in the present research is presented in Fig. 1. A rectangular FG beam with dimensions of dimensions in the *x* (length), *y* (width), and *z* (thickness) directions. It is hypothesized that material qualities differ continually across length and thickness directions. By grading ceramic and metal phases, a FG rectangular beam along the thickness is produced. Here, the lower side of beam ($z = -h/2$) is made of metal and the upper side ($z = +h/2$) is made of ceramic. Reference surface, or ($z = 0$), is the central axis of the beam. Origin (O) is the midpoint of a rectangular beam.

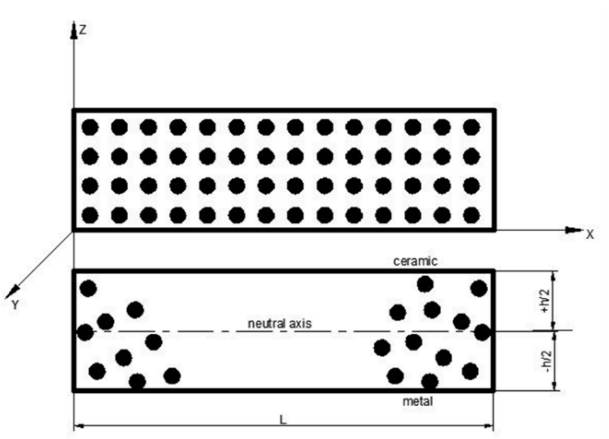

Fig. 1. Functionally graded beam geometry with even as well as uneven porosity

Material characteristics of FG beam depends on the volume proportion of their component materials. It is expected that the thickness coordinate and material characteristics have a functional relationship. A distribution of *x* and *z* values that follows power law could be used in representing the porous volume fraction (V_f) as shown in Eq. 1 [29].

$$V_f(x,z) = \left(\frac{x}{L}+\frac{1}{2}\right)^{P_x}\left(\frac{z}{h}+\frac{1}{2}\right)^{P_z} \quad (1)$$

here, P_z and P_x denote the behaviour of volume fraction throughout the thickness and length of beam.

Effective material properties in evenly distributed porous FG beams (P) can then be expressed in Eq. (2a) [28].

$$P(x,z) = P_m - \frac{\alpha}{2}(P_c + P_m) + (P_c - P_m)\left(\frac{x}{L}+\frac{1}{2}\right)^{P_x}\left(\frac{z}{h}+\frac{1}{2}\right)^{P_z} \quad (2a)$$

where α refers to porosity coefficient ($0 \le \alpha \le 1$), m is metal and c is ceramic.

2.2 Material homogenization

According to the aforementioned relationship, the Modulus of elasticity (E) and mass density (ρ), that are used for material stiffness and moment of inertia estimation for evenly distributed porous FG beams can be expressed in Eqs. (2b) and (2c) respectively [29].

$$E(x,z) = (E_c - E_m)\left(\frac{x}{L}+\frac{1}{2}\right)^{P_x}\left(\frac{z}{h}+\frac{1}{2}\right)^{P_z} + E_m - \frac{\alpha}{2}(E_c + E_m) \quad (2b)$$

$$\rho(x,z) = (\rho_c - \rho_m)\left(\frac{x}{L}+\frac{1}{2}\right)^{P_x}\left(\frac{z}{h}+\frac{1}{2}\right)^{P_z} + \rho_m - \frac{\alpha}{2}(\rho_c + \rho_m) \quad (2c)$$

Although a slight variance in Poisson's ratio is seen when compared with other properties, it is considered a constant because computations are made using the average value. Also, the effective properties of materials (P) for unevenly distributed porous FG beams could be estimated using Eq. (3a).

$$P(x,z) = (P_c - P_m)\left(\frac{x}{L}+\frac{1}{2}\right)^{P_x}\left(\frac{z}{h}+\frac{1}{2}\right)^{P_z} + P_m - \frac{\alpha}{2}(P_c + P_m)\left(1 - \frac{2|z|}{h}\right) \quad (3a)$$

The Modulus of elasticity (E), and mass density (ρ) for unevenly distributed porous FG beams could be estimated using Eqs. (3b) and (3c) respectively.

$$E(x,z) = (E_c - E_m)\left(\frac{z}{h}+\frac{1}{2}\right)^{P_z}\left(\frac{x}{L}+\frac{1}{2}\right)^{P_x} + E_m - \frac{\alpha}{2}(E_c + E_m)\left(1-\frac{2|z|}{h}\right) \quad (3b)$$

and

$$\rho(x,z) = (\rho_c - \rho_m)\left(\frac{z}{h}+\frac{1}{2}\right)^{P_z}\left(\frac{x}{L}+\frac{1}{2}\right)^{P_x} + \rho_m - \frac{\alpha}{2}(\rho_c + \rho_m)\left(1-\frac{2|z|}{h}\right) \quad (3c)$$

2.3 Constitutive equations for displacement field

To ensure rigid structure and lower manufacturing costs, FG beams and plates that experience static and dynamic loads must be well-designed. When analysing FGM structures that are adapted from conventional beam and plate theories, the results of the bending analysis often show that the deflections are underestimated, while the critical loads and natural frequencies are typically overstated. Therefore, it is advised to employ theories that consider shear deformation effects in FGB analysis so as to increase forecast accuracy. Reddy's advanced HSDT is adapted to find the effect of transverse shear. Displacement field and constitutive equations [30] are presented in Eqs. (4a) and (4b).

$$U(x,z,t) = u_0(x,t) + z\emptyset(x,t) - f(z)\left(\emptyset(x,t) + \frac{\partial w_0}{\partial x}(x,t)\right) \quad (4a)$$

$$W(x,z,t) = w_0(x,t) \quad (4b)$$

where U, and W are axial and transverse displacements. u_0 and w_0 are the axial and transverse displacements at a given point on the neutral axis. $\frac{\partial w_0}{\partial x}$ is the bending slope while $\emptyset$ is the shear slope. Displacement field equation in matrix form could be presented in Eq. (5),

$$\binom{U}{W} = \begin{bmatrix}1 & 0 & -z\\ 0 & 1 & 0\end{bmatrix}\{u_0 \quad w_0 \quad w_{0,x}\}^T = [z_d]\{d\} \quad (5)$$

The shear shape function f(z) could be applied to find transverse shear deformation as well as the non-zero strain field equations which can be computed using Eqs. (4a) and (4b) as,

$$\varepsilon_x = \frac{\partial U}{\partial x} = \frac{\partial u_0}{\partial x} - z\frac{\partial^2 w_0}{\partial x^2} + f(z)\left(\frac{\partial \emptyset}{\partial x} + \frac{\partial^2 w_0}{\partial x^2}\right) \quad (6a)$$

$$\varepsilon_z = \frac{\partial W}{\partial z} = 0 \quad (6b)$$

$$\gamma_{xz} = f'\left[\emptyset + \frac{\partial w_0}{\partial x}\right] \quad (6c)$$

and

$$f(z) = \frac{h}{\pi}sin\left[\frac{\pi z}{h}\right] - \frac{z}{\pi n}\left(1 - \frac{2}{nh}^{n-1} z^{n-1}\right) \quad (7a)$$

$$f'(z) = \frac{h}{\pi}sin\left[\frac{\pi}{h}\right] - \frac{1}{\pi n}\left(1 - \frac{2}{nh}^{n-1}(n-1)z^{n-2}\right) \quad (7b)$$

According to Hooke's Law and using Eqs. (6a), (6b), (6c), (7a), and (7b), the field equations for stress can be deduced as shown in Eqs. (8a) and (8b).

$$\sigma_x = \frac{E(x,z)}{1-\mu^2}\varepsilon_x \quad (8a)$$

and

$$\tau_{xz} = \frac{E(x,z)}{2(1+\mu)}\gamma_{xz} \quad (8b)$$

2.4 Equations of motion

One of the most important concepts in vibration analysis is Hamilton's principle. It results in the fundamental equations of elasticity and dynamics, which are given in Eq. (9) [29].

$$\int_{t1}^{t2}(\delta U + \delta V - \delta K)\,dt = 0 \quad (9)$$

where t_1 and t_2 are the beginning and the end points in time. δU, δV, and δK represent changes in strain energy, potential energy, and kinetic energy respectively. The change in strain energy in a 2D-FGPB can be expressed in Eq. (10).

$$U = \frac{1}{2}\int_0^L\int_{-\frac{h}{2}}^{+\frac{h}{2}}(\sigma_x\varepsilon_x + \tau_{xz}\gamma_{xz})dzdx \quad (10)$$

substituting Eqs. (6a), (6c), (8a), and (8b) into Eq. (10), strain energy could be deduced as,

$$\mathrm{U} = \frac{1}{2}\int_0^{\mathrm{L}}\int_{-\frac{\mathrm{h}}{2}}^{+\frac{\mathrm{h}}{2}}\left[\left(\frac{\mathrm{E(x,z)}}{1-\mu^2}\left(\left(\frac{\partial u_0}{\partial x}\right)^2 - 2\mathrm{f}\frac{\partial u_0}{\partial x}\frac{\mathrm{d}^2 w_0}{\mathrm{dx}^2} + (2\mathrm{z} - 2\mathrm{f})\frac{\partial u_0}{\partial x}\frac{\partial \phi}{\partial x} + \mathrm{f}^2\left(\frac{\mathrm{d}^2 w_0}{\mathrm{dx}^2}\right)^2 + \frac{\mathrm{d}^2 w_0}{\mathrm{dx}^2}\frac{\partial \phi}{\partial x}(2\mathrm{f}^2 - 2\mathrm{zf}) + \left(\frac{\partial \phi}{\partial x}\right)^2(\mathrm{z}^2 - 2\mathrm{zf} + \mathrm{f}^2)\right)\right) + \frac{\mathrm{E(x,z)}}{2(1+\mu)}\left(\phi^2(1 - 2\mathrm{f}' + (\mathrm{f}')^2 + \phi\frac{\partial w_0}{\partial x}(2 - 4\mathrm{f}'^{-}2\mathrm{f}'^{2}) + \left(\frac{\mathrm{dw}_0}{\mathrm{dx}}\right)^2(1 - 2\mathrm{f}' - (\mathrm{f}')^2)\right)\right]\mathrm{dzdx} \quad (11a)$$

$$\mathrm{U} = \frac{1}{2}\int_0^{\mathrm{L}}\int_{-\frac{\mathrm{h}}{2}}^{+\frac{\mathrm{h}}{2}}\left[\left(\frac{\mathrm{E(x,z)}}{1-\mu^2}\left(\mathrm{A}\left(\frac{\partial u_0}{\partial x}\right)^2 - 2\mathrm{D}\frac{\partial u_0}{\partial x}\frac{\mathrm{d}^2 w_0}{\mathrm{dx}^2} + (2\mathrm{B} - 2\mathrm{D})\frac{\partial u_0}{\partial x}\frac{\partial \phi}{\partial x} + \mathrm{H}\left(\frac{\mathrm{d}^2 w_0}{\mathrm{dx}^2}\right)^2 + \frac{\mathrm{d}^2 w_0}{\mathrm{dx}^2}\frac{\partial \phi}{\partial x}(2\mathrm{H} - 2\mathrm{BD}) + \left(\frac{\partial \phi}{\partial x}\right)^2(\mathrm{C} - 2\mathrm{BD} + \mathrm{H})\right)\right) + \frac{\mathrm{E(x,z)}}{2(1+\mu)}\left(\phi^2(1 - 2\mathrm{C} + \mathrm{H}) + \phi\frac{\partial w_0}{\partial x}(2 - 4\mathrm{C} - 2\mathrm{F}) + \left(\frac{\mathrm{dw}_0}{\mathrm{dx}}\right)^2(1 - 2\mathrm{C} - \mathrm{F})\right)\right]\mathrm{dx} \quad (11b)$$

and,

$$(\mathrm{A,B,C,D,F,H}) = \int_{-\frac{\mathrm{h}}{2}}^{+\frac{\mathrm{h}}{2}}(1, \mathrm{z}, \mathrm{f}', \mathrm{f}, (\mathrm{f}')^2, (\mathrm{f})^2)\mathrm{dz} \quad (11c)$$

where A,B,C,D, F, and H are stress resultants.

The variation in potential energy while applying transverse load q could be expressed as shown in Eq. (12).

$$\delta V = -\int_0^L q\delta(w_b + w_s)dx \quad (12)$$

Variation in kinetic energy of a 2D- FGPB could be presented as in Eq. (13a).

$$K = \frac{1}{2}\int_0^L\int_{-\frac{h}{2}}^{+\frac{h}{2}}\left[\left(\rho(\mathrm{x},z)\frac{\mathrm{E(x,z)}}{1-\mu^2}\left(I_0\left(\frac{\partial u_0}{\partial t}\right)^2 - 2J_1\frac{\partial u_0}{\partial t}\frac{d^2 w_0}{dxdt} + (2I_1 - 2J_1)\frac{\partial u_0}{\partial t}\frac{\partial \phi}{\partial t} + K_1\left(\frac{d^2 w_0}{\partial xdt}\right)^2 + (2I_1 - 2I_1J_1)\frac{d^2 w_0}{dxdt}\frac{\partial \phi}{\partial t} + (I_2 - 2I_1J_1 + K_1)\left(\frac{\partial \phi}{\partial t}\right)^2\right)\right) + \rho(\mathrm{x},z)\frac{\mathrm{E(x,z)}}{2(1+\mu)}\left(\phi^2(1 - 2I_2 +$$

$$K_1) + \phi \frac{\partial w_0}{\partial t}(2 - 4I_2 - 2J_2) + \left(\frac{d^2 w_0}{dxdt}\right)^2 (1 - 2I_2 - J_2)\Big)\Big] dx \quad (13a)$$

$$(\mathrm{I_0}, \mathrm{I_1}, \mathrm{I_2}, \mathrm{J_1}, \mathrm{J_2}, \mathrm{K_1}) = \int_{-\frac{\mathrm{h}}{2}}^{+\frac{\mathrm{h}}{2}} (1, \mathrm{z}, \mathrm{f}', \mathrm{f}, (\mathrm{f}')^2, (\mathrm{f})^2) \quad (13b)$$

where $\mathrm{I_0}, \mathrm{I_1}, \mathrm{I_2}, \mathrm{J_1}, \mathrm{J_2}, \mathrm{K_1}$ are mass inertias.

when functions, $u_0(x,t)$, $w_0(x,t)$ and $\phi(x,t)$, of infinite dimensions are expressed as generalised coordinates. As a result, the displacement functions are represented by a polynomial series and are presented in Tab. 1 [23, 29].

Table 1. Different kinematic constraints that are used in numerical calculations

Boundary condition	**X = -L/2**	**x = L/2**
Simply supported (SS)	u=0, w=0	w=0
Clamped-clamped (CC)	u=0, w=0, ϕ=0, w'=0	u=0,w=0, ϕ=0, w'=0
Clamped- free (CF)	u=0, w=0, ϕ=0, w'=0	---

Substituting Eqs. (11b), (12), and (13a) into Eq. (9) and integrating with respect to time intervals, the displacement function coefficients are expressed as shown in Eqs. (14a), (14b), and (14c).

$$u_0(x,t) = \sum_{j=1}^{m} A_j \theta_j(x) e^{i\omega t}, \quad \theta_j(x) = \left(x + \frac{L}{2}\right)^{p_u} \left(x - \frac{L}{2}\right)^{q_u} x^{m-1} \quad (14a)$$

$$w_0(x,t) = \sum_{j=1}^{m} B_j \varphi_j(x) e^{i\omega t}, \quad \varphi_j(x) = \left(x + \frac{L}{2}\right)^{p_w} \left(x - \frac{L}{2}\right)^{q_w} x^{m-1} \quad (14b)$$

$$\phi(x,t) = \sum_{j=1}^{m} C_j \psi_j(x) e^{i\omega t}, \quad \psi_j(x) = \left(x + \frac{L}{2}\right)^{p_\phi} \left(x - \frac{L}{2}\right)^{q_\phi} x^{m-1} \quad (14c)$$

where, $\theta_j(x)$, $\varphi_j(x)$, and $\psi_j(x)$ are shape functions for boundary conditions. A_j, B_j, and C_j are unknown coefficients that are to be estimated. ω is the natural frequency. p_u, q_u, p_w, q_w, p_ϕ, q_ϕ are the boundary exponents and the values for boundary exponents can be taken from Table 2 [23].

Table 2. Boundary exponents to be used for boundary conditions

Boundary condition	Left end			Right end		
	p_u	p_w	p_ϕ	q_u	q_w	q_ϕ
SS	1	1	0	0	1	0
CC	1	2	1	1	2	1
CF	1	2	1	0	0	0

Substituting Eqs. (14a), (14b), and (14c) into Eqs. (11a) and (13a), governing equation of motion could be derived as shown in Eq. (15).

$$\frac{\partial \mathrm{U}}{\partial \mathrm{q_j}} + \frac{\partial}{\mathrm{dt}}\left(\frac{\partial \mathrm{k}}{\partial \mathrm{q_j}}\right) = 0 \quad (15)$$

Further, the analytical solutions could be obtained using the following expression as shown in Eq. (16) [32].

$$\begin{bmatrix} [S_{11}] & [S_{12}] & [S_{13}] \\ [S_{12}]^T & [S_{22}] & [S_{23}] \\ [S_{13}]^T & [S_{23}]^T & [S_{33}] \end{bmatrix} - \omega^2 \begin{bmatrix} [M_{11}] & [M_{12}] & [M_{13}] \\ [M_{12}]^T & [M_{22}] & [M_{23}] \\ [M_{13}]^T & [M_{23}]^T & [M_{33}] \end{bmatrix} \begin{Bmatrix} A \\ B \\ C \end{Bmatrix} = \begin{Bmatrix} \{0\} \\ \{0\} \\ \{0\} \end{Bmatrix} \quad (16)$$

where,

$$S_{11}(i,j) = \mathrm{A} \int_{-\frac{L}{2}}^{\frac{L}{2}} \frac{E(x,z)}{1-\mu^2} \theta_{i,x} \theta_{j,x} dx \quad (17)$$

$$S_{12}(i,j) = -D \int_{-\frac{L}{2}}^{\frac{L}{2}} \frac{E(x,z)}{1-\mu^2} \theta_{i,x} \varphi_{j,xx} dx \quad (18)$$

$$S_{13}(i,j) = (B - D) \int_{-\frac{L}{2}}^{\frac{L}{2}} \frac{E(x,z)}{1-\mu^2} \theta_{i,x} \psi_{j,x} dx \quad (19)$$

$$S_{22}(i,j) = \mathrm{H} \int_{-\frac{L}{2}}^{\frac{L}{2}} \frac{E(x,z)}{1-\mu^2} \varphi_{i,xx} \varphi_{j,xx}\, dx + (1 - 2\mathrm{C} - \mathrm{F}) \int_{-\frac{L}{2}}^{\frac{L}{2}} \frac{E(x,z)}{2(1+\mu)} \quad (20)$$

$$\varphi_{i,x} \varphi_{j,x} dx \quad (21)$$

$$S_{23}(i,j) = (2\mathrm{H} - 2\mathrm{BD}) \int_{-\frac{L}{2}}^{\frac{L}{2}} \frac{E(x,z)}{1-\mu^2} \varphi_{i,xx} \psi_{j,x} dx + (2 - 4I_2 - 2J_2) \int_{-\frac{L}{2}}^{\frac{L}{2}} \frac{E(x,z)}{2(1+\mu)} \quad (22)$$

$$S_{33}(i,j) = \mathrm{C} - 2\mathrm{BD} + \mathrm{H} \int_{-\frac{L}{2}}^{\frac{L}{2}} \frac{E(x,z)}{1-\mu^2} \psi_{i,x} \psi_{j,x} dx + (1 - 2\mathrm{C} + \mathrm{H}) \int_{-\frac{L}{2}}^{\frac{L}{2}} \frac{E(x,z)}{2(1+\mu)} \psi_i \psi_j dx \quad (23)$$

$$M_{11}(i,j) = I_0 \int_{-L/2}^{L/2} \rho(x,z) \frac{\mathrm{E(x,z)}}{1-\mu^2} \theta_i \theta_j dx \quad (24)$$

$$M_{12}(i,j) = -2J_1 \int_{-L/2}^{L/2} \rho(z) \frac{\mathrm{E(x,z)}}{1-\mu^2} \theta_i \varphi_{j,x} dx \quad (25)$$

$$M_{13}(i,j) = 2I_1 - 2J_1 \int_{-L/2}^{L/2} \rho(x,z) \frac{\mathrm{E(x,z)}}{1-\mu^2} \theta_i \psi_j dx \quad (26)$$

$$M_{22}(i,j) = K_1 \int_{-\frac{L}{2}}^{\frac{L}{2}} \rho(x,z) \frac{\mathrm{E(x,z)}}{1-\mu^2} \varphi_i \varphi_j dx + (1 - 2I_2 - J_2) \int_{-\frac{L}{2}}^{\frac{L}{2}} \rho(x,z) \frac{E(x,z)}{2(1+\mu)} \varphi_{i,x} \varphi_{j,x} dx \quad (27)$$

$$M_{23}(i,j) = 2I_1 - 2I_1 J_1 \int_{-\frac{L}{2}}^{\frac{L}{2}} \rho(x,z) \frac{\mathrm{E(x,z)}}{1-\mu^2} \varphi_{i,x} \psi_j dx \quad (28)$$

$$M_{33}(i,j) = (I_2 - 2I_1 J_1 + K_1) \int_{-\frac{L}{2}}^{\frac{L}{2}} \rho(x,z) \frac{E(x,z)}{1-\mu^2} \psi_i \psi_j dx \quad (29)$$

3. Results and Discussion

3.1 Effect of gradation on natural frequency

To determine the accuracy of the proposed theory in calculating natural frequencies, a 2D- FGPB is considered whose length varies from –L to +L and thickness varies as –h/2 to +h/2. The constituents of beam [29] are Al/Al_2O_3, and the properties are Alumina: $E_c = 380$ GPa, $\rho_c = 3960\ kg/m^3$, $\mu_c = 0.3$; Aluminum: $E_m = 70$ GPa, $\rho_m = 2702\ kg/m^3$, $\mu_m = 0.3$

A dimensionless natural frequency (λ) could be used to represent the results using the Eq. (30).

$$\lambda = \frac{\omega L^2}{h}\sqrt{\frac{\rho_m}{E_m}} \tag{30}$$

A homogeneous beam is taken into account for the convergence and verification investigations, and displacement functions having various terms (m = 2, 4, 6, 8, 10, and 12) have been used [31]. Calculated findings are provided as a dimensionless free vibration, taking into account different gradient index values in both directions. For comparison, findings from the earlier investigations [27, 29] for dimensionless free vibration are detailed in Tabs. 3 - 8 for the mentioned SS, CC, and CF boundary conditions at L/h = 5 and L/h = 20.

Table 3. Influence of p_x, and p_z, on λ for a SS 2D-FGPB at L/h = 5

Beam Theory		P_x	P_z					
			0.0	**0.2**	**0.4**	**0.6**	**0.8**	**1.0**
[23]		0.0	2.677	2.677	2.677	2.677	2.677	2.677
[28]			2.676	2.674	2.666	2.653	2.633	2.610
[29]			2.677	2.675	2.666	2.654	2.635	2.612
PRESENT	2 terms		2.553	2.529	2.505	2.481	2.457	2.433
	4 terms		2.476	2.452	2.428	2.404	2.380	2.356
	6 terms		2.399	2.375	2.351	2.327	2.303	2.279
	8 terms		2.323	2.299	2.275	2.251	2.227	2.203
	10 terms		2.323	2.299	2.275	2.251	2.227	2.203
	12 terms		2.323	2.299	2.275	2.251	2.227	2.203
[23]		0.5	2.672	2.672	2.672	2.672	2.672	2.672
[28]			2.672	2.672	2.672	2.672	2.672	2.672
[29]			2.673	2.670	2.662	2.648	2.629	2.606
PRESENT	2 terms		2.478	2.475	2.467	2.453	2.434	2.412
	4 terms		2.400	2.397	2.389	2.375	2.356	2.333
	6 terms		2.321	2.318	2.310	2.296	2.277	2.255
	8 terms		2.321	2.318	2.310	2.296	2.277	2.255
	10 terms		2.321	2.318	2.310	2.296	2.277	2.255
	12 terms		2.321	2.318	2.310	2.296	2.277	2.255
[23]		1.0	2.645	2.645	2.645	2.645	2.645	2.645
[28]			2.645	2.645	2.645	2.645	2.645	2.645
[29]			2.645	2.642	2.634	2.621	2.603	2.579
PRESENT	2 terms		2.413	2.410	2.402	2.389	2.371	2.347
	4 terms		2.389	2.385	2.377	2.364	2.346	2.323
	6 terms		2.365	2.361	2.353	2.340	2.322	2.299
	8 terms		2.365	2.361	2.353	2.340	2.322	2.299
	10 terms		2.365	2.361	2.353	2.340	2.322	2.299
	12 terms		2.365	2.361	2.353	2.340	2.322	2.299

Table 4. The effect of p_x and p_z on the value of λ for a CC 2D-FGPB with L/h = 5

Beam Theory		P_x	P_z					
			0.0	**0.2**	**0.4**	**0.6**	**0.8**	**1.0**
[23]		0.0	5.194	5.194	5.194	5.194	5.194	5.194
[28]			5.231	5.231	5.231	5.231	5.231	5.231
[29]			5.233	5.230	5.221	5.206	5.184	5.156
PRESENT	2 terms		5.212	5.209	5.200	5.184	5.163	5.135
	4 terms		5.190	5.187	5.178	5.163	5.142	5.114
	6 terms		5.169	5.166	5.157	5.142	5.120	5.093
	8 terms		5.169	5.166	5.157	5.142	5.120	5.093
	10 terms		5.169	5.166	5.157	5.142	5.120	5.093
	12 terms		5.169	5.166	5.157	5.142	5.120	5.093
[23]		0.5	5.198	5.198	5.198	5.198	5.198	5.198
[28]			5.237	5.237	5.237	5.237	5.237	5.237
[29]			5.238	5.235	5.226	5.216	5.189	5.161
PRESENT	2 terms		5.205	5.202	5.193	5.177	5.156	5.128
	4 terms		5.183	5.180	5.171	5.156	5.135	5.107
	6 terms		5.162	5.159	5.150	5.135	5.113	5.086
	8 terms		5.162	5.159	5.150	5.135	5.113	5.086
	10 terms		5.162	5.159	5.150	5.135	5.113	5.086
	12 terms		5.162	5.159	5.150	5.135	5.113	5.086
[23]		1.0	5.219	5.219	5.219	5.219	5.219	5.219
[28]			5.258	5.258	5.258	5.258	5.258	5.258
[29]			5.263	5.260	5.251	5.236	5.214	5.186
PRESENT	2 terms		5.201	5.198	5.189	5.173	5.152	5.124
	4 terms		5.179	5.176	5.167	5.152	5.131	5.103
	6 terms		5.158	5.155	5.146	5.131	5.109	5.082
	8 terms		5.158	5.155	5.146	5.131	5.109	5.082
	10 terms		5.158	5.155	5.146	5.131	5.109	5.082
	12 terms		5.158	5.155	5.146	5.131	5.109	5.082

Table 5. The effect of p_x and p_z on the value of λ for a CF 2D-FGPB with L/h = 5

Beam Theory		P_x	P_z					
			0.0	**0.2**	**0.4**	**0.6**	**0.8**	**1.0**
[23]		0.0	0.984	0.984	0.984	0.984	0.984	0.984
[28]			0.984	0.984	0.984	0.984	0.984	0.984
[29]			0.985	0.984	0.981	0.977	0.971	0.963
PRESENT	2 terms		0.951	0.950	0.947	0.943	0.937	0.929
	4 terms		0.917	0.916	0.913	0.909	0.903	0.895
	6 terms		0.883	0.882	0.879	0.875	0.869	0.861
	8 terms		0.883	0.882	0.879	0.875	0.869	0.861
	10 terms		0.883	0.882	0.879	0.875	0.869	0.861
	12 terms		0.883	0.882	0.879	0.875	0.869	0.861
[23]		0.5	0.870	0.870	0.870	0.870	0.870	0.870
[28]			0.872	0.872	0.872	0.872	0.872	0.872
[29]			0.871	0.870	0.867	0.863	0.851	0.849
PRESENT	2 terms		0.859	0.859	0.856	0.852	0.840	0.838
	4 terms		0.848	0.847	0.845	0.841	0.828	0.827
	6 terms		0.837	0.836	0.834	0.830	0.817	0.816
	8 terms		0.837	0.836	0.834	0.830	0.817	0.816
	10 terms		0.837	0.836	0.834	0.830	0.817	0.816
	12 terms		0.837	0.836	0.834	0.830	0.817	0.816
[23]		1.0	0.721	0.721	0.721	0.721	0.721	0.721
[28]			0.722	0.722	0.722	0.722	0.722	0.722
[29]			0.723	0.722	0.720	0.716	0.712	0.706
PRESENT	2 terms		0.706	0.706	0.704	0.700	0.696	0.690
	4 terms		0.690	0.690	0.688	0.684	0.680	0.674
	6 terms		0.674	0.674	0.672	0.668	0.664	0.658
	8 terms		0.674	0.674	0.672	0.668	0.664	0.658
	10 terms		0.674	0.674	0.672	0.668	0.664	0.658
	12 terms		0.674	0.674	0.672	0.668	0.664	0.658

Table 6. The effect of p_x and p_z on the value of λ for a SS 2D-FGPB with L/h = 20

Beam Theory		P_x	P_z					
			0.0	**0.2**	**0.4**	**0.6**	**0.8**	**1.0**
[23]		0.0	2.836	2.836	2.836	2.836	2.836	2.836
[28]			2.837	2.837	2.837	2.837	2.837	2.837
[29]			2.837	2.834	2.826	2.812	2.792	2.768
PRESENT	2 terms		2.795	2.792	2.784	2.770	2.750	2.726
	4 terms		2.753	2.750	2.741	2.728	2.708	2.684
	6 terms		2.711	2.708	2.699	2.685	2.666	2.642
	8 terms		2.711	2.708	2.699	2.685	2.666	2.642
	10 terms		2.711	2.708	2.699	2.685	2.666	2.642
	12 terms		2.711	2.708	2.699	2.685	2.666	2.642
[23]		0.5	2.833	2.833	2.833	2.833	2.833	2.833
[28]			2.832	2.832	2.832	2.832	2.832	2.832
[29]			2.833	2.830	2.821	2.807	2.788	2.764
PRESENT	2 terms		2.789	2.786	2.778	2.764	2.744	2.720
	4 terms		2.747	2.744	2.735	2.722	2.702	2.678
	6 terms		2.705	2.702	2.693	2.679	2.660	2.636
	8 terms		2.705	2.702	2.693	2.679	2.660	2.636
	10 terms		2.705	2.702	2.693	2.679	2.660	2.636
	12 terms		2.705	2.702	2.693	2.679	2.660	2.636
[23]		1.0	2.809	2.809	2.809	2.809	2.809	2.809
[28]			2.808	2.808	2.808	2.808	2.808	2.808
[29]			2.809	2.806	2.798	2.784	2.765	2.741
PRESENT	2 terms		2.781	2.778	2.770	2.756	2.736	2.712

R	4 terms		2.739	2.736	2.727	2.714	2.694	2.670
E	6 terms		2.697	2.694	2.685	2.671	2.652	2.628
S	8 terms		2.697	2.694	2.685	2.671	2.652	2.628
E	10 terms		2.697	2.694	2.685	2.671	2.652	2.628
N	12 terms		2.697	2.694	2.685	2.671	2.652	2.628
T								

Table 7. The effect of p_x and p_z on the value of λ for a CC 2D-FGPB with L/h = 20

Beam theory		P_x	P_z					
			0.0	**0.2**	**0.4**	**0.6**	**0.8**	**1.0**
[23]		0.0	6.348	6.348	6.348	6.348	6.348	6.348
[28]			5.133	5.133	5.133	5.133	5.133	5.133
[29]			6.351	6.345	6.327	6.297	6.256	6.203
P	2 terms		6.338	6.332	6.314	6.284	6.243	6.190
R	4 terms		6.325	6.319	6.301	6.271	6.229	6.177
E	6 terms		6.312	6.306	6.288	6.258	6.216	6.164
S	8 terms		6.312	6.306	6.288	6.258	6.216	6.164
E	10 terms		6.312	6.306	6.288	6.258	6.216	6.164
N	12 terms		6.312	6.306	6.288	6.258	6.216	6.164
T								
[23]		0.5	5.112	5.112	5.112	5.112	5.112	5.112
[28]			5.138	5.138	5.138	5.138	5.138	5.138
[29]			6.358	6.352	6.333	6.303	6.262	6.209
P	2 terms		6.287	6.281	6.263	6.233	6.192	6.139
R	4 terms		6.274	6.268	6.250	6.220	6.178	6.126
E	6 terms		6.261	6.255	6.237	6.207	6.165	6.113
S	8 terms		6.261	6.255	6.237	6.207	6.165	6.113
E	10 terms		6.261	6.255	6.237	6.207	6.165	6.113
N	12 terms		6.261	6.255	6.237	6.207	6.165	6.113
T								
[23]		1.0	5.133	5.133	5.133	5.133	5.133	5.133
[28]			5.160	5.160	5.160	5.160	5.160	5.160
[29]			6.391	6.384	6.366	6.336	6.294	6.241
P	2 terms		6.283	6.277	6.259	6.229	6.188	6.135
R	4 terms		6.270	6.264	6.246	6.216	6.174	6.122
E	6 terms		6.257	6.251	6.233	6.203	6.161	6.109
S	8 terms		6.257	6.251	6.233	6.203	6.161	6.109
E	10 terms		6.257	6.251	6.233	6.203	6.161	6.109
N	12 terms		6.257	6.251	6.233	6.203	6.161	6.109
T								

Table 8. The effect of p_x and p_z on the value of λ for a CF 2D-FGPB with L/h = 20

Beam Theory		P_x	P_z					
			0.0	**0.2**	**0.4**	**0.6**	**0.8**	**1.0**
[23]		0.0	1.012	1.012	1.012	1.012	1.012	1.012
[28]			1.013	1.013	1.013	1.013	1.013	1.013
[29]			1.013	1.012	1.009	1.004	0.997	0.989
P	2 terms		0.992	0.991	0.988	0.983	0.976	0.968
R	4 terms		0.971	0.970	0.967	0.962	0.955	0.947
E	6 terms		0.950	0.949	0.946	0.941	0.934	0.926
S	8 terms		0.950	0.949	0.946	0.941	0.934	0.926
E	10 terms		0.950	0.949	0.946	0.941	0.934	0.926
N	12 terms		0.950	0.949	0.946	0.941	0.934	0.926
T								
[23]		0.5	0.895	0.895	0.895	0.895	0.895	0.895
[28]			0.895	0.895	0.895	0.895	0.895	0.895
[29]			0.895	0.894	0.891	0.887	0.881	0.873
P	2 terms		0.884	0.883	0.880	0.876	0.870	0.862
R	4 terms		0.873	0.872	0.869	0.865	0.859	0.851
E	6 terms		0.862	0.861	0.858	0.854	0.848	0.840
S	8 terms		0.862	0.861	0.858	0.854	0.848	0.840
E	10 terms		0.862	0.861	0.858	0.854	0.848	0.840
N	12 terms		0.862	0.861	0.858	0.854	0.848	0.840
T								
[23]		1.0	0.739	0.739	0.739	0.739	0.739	0.739
[28]			0.739	0.739	0.739	0.739	0.739	0.739
[29]			0.739	0.739	0.736	0.733	0.728	0.721
P	2 terms		0.728	0.727	0.725	0.721	0.716	0.710
R	4 terms		0.717	0.716	0.714	0.710	0.705	0.699
E	6 terms		0.706	0.705	0.703	0.699	0.694	0.688
S	8 terms		0.706	0.705	0.703	0.699	0.694	0.688
E	10 terms		0.706	0.705	0.703	0.699	0.694	0.688
N	12 terms		0.706	0.705	0.703	0.699	0.694	0.688
T								

Dimensionless free vibration of SS, CC, and CF beams showed rapid reaction and polynomial expansion of 6 in SS and 4 in CC and CF. However, a 12-term polynomial expansion was evaluated for accuracy. As gradient indices increase in both directions, dimensionless free vibration diminishes in SS, CC, and CF beams with aspect ratios of L/h = 5 and 20. As the gradient index value increases, the natural frequency in the CC beam increases in the *x* direction while it decreases along the *z* direction, influenced by the end constraints and reactions. Gradient index improve beam stiffness and elasticity modulus [21]. Gradient indices, elasticity modulus, and beam stiffness increase frequencies. This is accurate if the beam's mass remains constant. Vibration theory states that mass inversely affects frequency and stiffness directly affects frequency. As demonstrated in Tabs. 5 and 6, gradient indexes have the same influence on SS and CC beam frequencies, but *x*- direction index is much more effective than *z*- direction index [23]. Gradient index affects frequency more in *z* than in *x* in CF beams. As seen in Tabs. 3 to 8, the CC beam exhibits highest frequency, followed by the SS and CF beams. The aspect ratio effect is crucial because free vibration increases as aspect ratio increases (Figs. 2, 3, and 4).

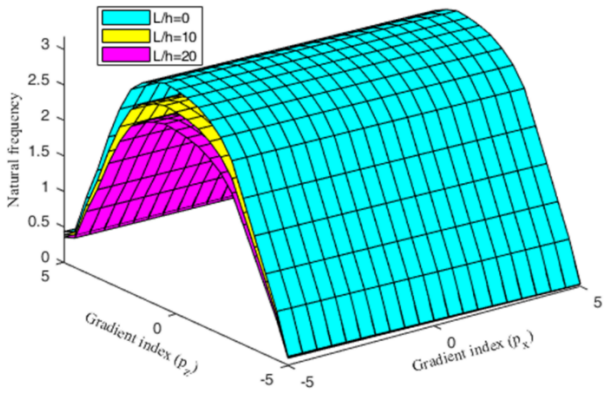

Fig. 2. Variation in natural frequencies of SS beam with respect to aspect ratios along p_x and p_z

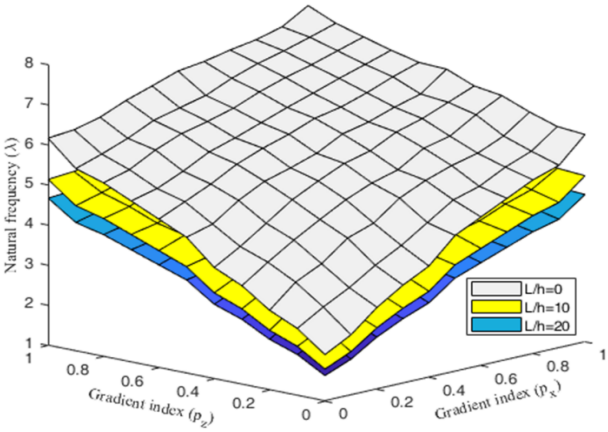

Fig. 3. Variation in natural frequencies of CC beam with respect to aspect ratios along p_x and p_z

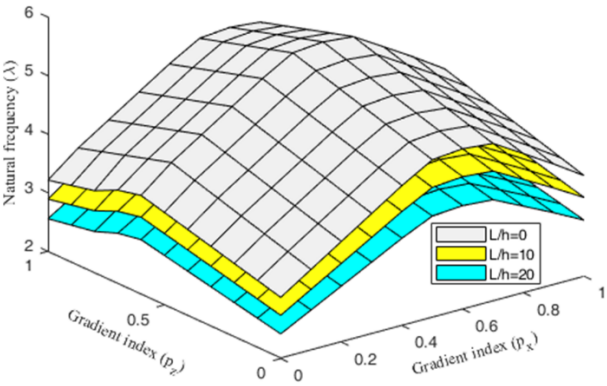

Fig. 4. Variation in natural frequencies of CF beam with respect to aspect ratios along p_x and p_z

The beam's stiffness and mass depend on the material's characteristics and cross-section geometry, while its gradation exponent and gradient index affect its natural frequency. An increase in the gradation exponent increases the beam's rigidity, resulting in a higher natural frequency. Conversely, an increase in the gradient index increases stiffness and natural frequency, resulting in a higher natural frequency. However, the gradient index's impact on the natural frequency of a CF beam is less significant compared to SS and CC boundary conditions. The aspect ratio of an SS 2D-FGPB can significantly affect its natural oscillation frequency. It reduces the beam's mass and cross-sectional area, but the increase in rigidity due to beam lengthening increases its natural frequency. The increase in aspect ratio leads to increased beam length [33], increased rigidity, and higher natural frequency. However, this decrease in cross-sectional area results in a decrease in mass and frequency. To compensate, beam thickness is increased.

3.2 Effect of porosity on natural frequency

The effect on material gradation and porosity distribution, even and uneven, is presented in this section. The variations in natural frequencies in a 2D-FGPB with even porosity for the considered boundary conditions SS, CC, and CF are presented in Tabs. 9, 10, and 11 and subsequently in Figs. 5 to 10. The porosity of a 2D-FGPB decreases its natural frequency due to cavities or pores, affecting its resistance to deformation and oscillation. The distribution of mass and rigidity also affects the frequency. A uniform distribution reduces stress concentrations and increases resistance. An uneven distribution increases frequency, as tension concentrations in specific regions contribute to higher stiffness and frequency [34]. In contrast to an SS beam, CC boundary conditions impose a fixed boundary at each extremity of the beam, resulting in distinct mode shapes and natural frequencies. At the locations where an SS beam is supported, the beam is free to move up and down [35]. This means that the support points can function as locations of maximum displacement and minimum bending moment, resulting in a beam with a reduced effective stiffness. The decline in effective rigidity reduces the natural frequency. A CC beam, on the other hand, is stationary at both ends. This indicates that there is no movement at the support points, and that the greatest displacement occurs in the center of the beam. Fixed boundary conditions increase the effective rigidity of the beam, thereby increasing its natural frequency. Moreover, the mode shapes of the beam can vary between the two boundary conditions. In an SS beam, the mode morphologies have a maximum amplitude at the beam's center, whereas in a CC beam, there is a node. The natural frequency of a beam can also be affected by the mode shape. As the porosity increases, the effective stiffness and mass of the composite beam decrease, which results in a decrease in its natural frequency. This effect can be more predominant for aluminum than for alumina due to the larger difference in their stiffness and density.

Table 9. Effect of p_x, p_z and α on natural frequencies of SS 2D-FGPB at the aspect ratio of L/h=5

P_x & P_z	Even Porosity				Uneven Porosity			
	0.0	0.1	0.2	0.3	0.0	0.1	0.2	0.3
0.0	2.6753	2.776	2.8172	2.8507	2.6753	2.7561	2.7792	2.7934
0.2	2.6717	2.7687	2.8061	2.8355	2.6717	2.7522	2.7754	2.7893
0.4	2.6594	2.7538	2.7876	2.8133	2.6594	2.7402	2.7598	2.772
0.6	2.6426	2.7312	2.7607	2.784	2.6426	2.7177	2.7369	2.7473
0.8	2.6171	2.7011	2.7284	2.7478	2.6171	2.6886	2.7059	2.7145
1.0	2.5771	2.6635	2.688	2.7047	2.5771	2.6519	2.6672	2.6742

Table 10. Effect of p_x, p_z and α on natural frequencies of CC 2D-FGPB at the aspect ratio of L/h=5

P_x & P_z	Even Porosity				Uneven Porosity			
	0.0	0.1	0.2	0.3	0.0	0.1	0.2	0.3
0.0	5.1618	5.5842	5.9157	6.2572	5.1618	5.5539	5.8465	6.1400
0.2	5.1600	5.5160	5.8988	6.2295	5.1600	5.4913	5.8417	6.1330
0.4	5.1545	5.5035	5.8769	6.1965	5.1545	5.4827	5.8285	6.1144
0.6	5.1453	5.4868	5.8502	6.1583	5.1453	5.4688	5.8081	6.0867
0.8	5.1322	5.4658	5.8186	6.1150	5.1322	5.4499	5.7813	6.0514
1.0	5.1152	5.4404	5.7822	6.0666	5.1152	5.4261	5.7487	6.0094

Table 11. Effect of p_x, p_z and α on natural frequencies of CF 2D-FGPB at the aspect ratio of L/h=5

P_x & P_z	Even Porosity				Uneven Porosity			
	0.0	0.1	0.2	0.3	0.0	0.1	0.2	0.3
0.0	0.9850	1.0006	1.0142	1.0256	0.9850	0.9944	1.0014	1.0057
0.2	0.9255	0.9381	0.9488	0.9571	0.9255	0.9317	0.9355	0.9364
0.4	0.8673	0.8777	0.8861	0.8922	0.8673	0.8714	0.8731	0.8720
0.6	0.8108	0.8193	0.8260	0.8305	0.8108	0.8134	0.8137	0.8114
0.8	0.7560	0.7631	0.7685	0.7718	0.7560	0.7576	0.7571	0.7542
1.0	0.7059	0.7092	0.7135	0.7160	0.7059	0.7042	0.7032	0.7000

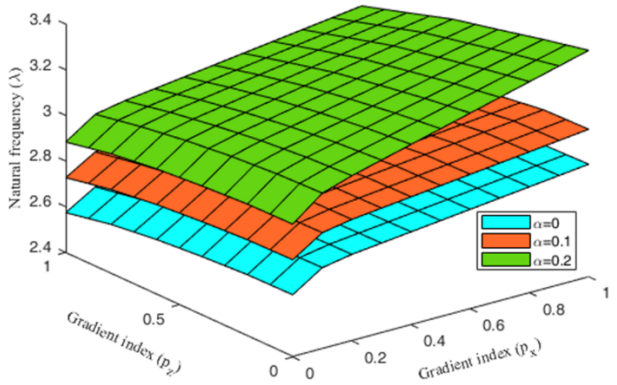

Fig. 5. Effect of α on λ for SS 2D-FGPB with even porosity at the aspect ratio of L/h=5

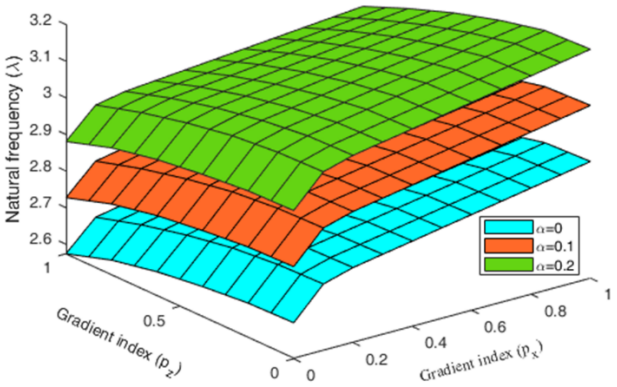

Fig. 6. Effect of α on λ for SS 2D-FGPB with un-even porosity at the aspect ratio of L/h=5

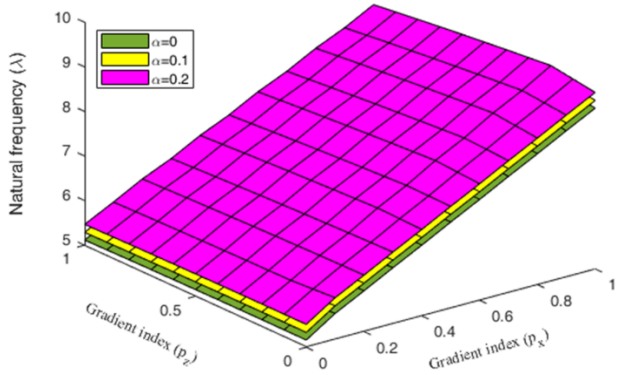

Fig. 7. Effect of α on λ for CC 2D-FGPB with even porosity at the aspect ratio of L/h=5

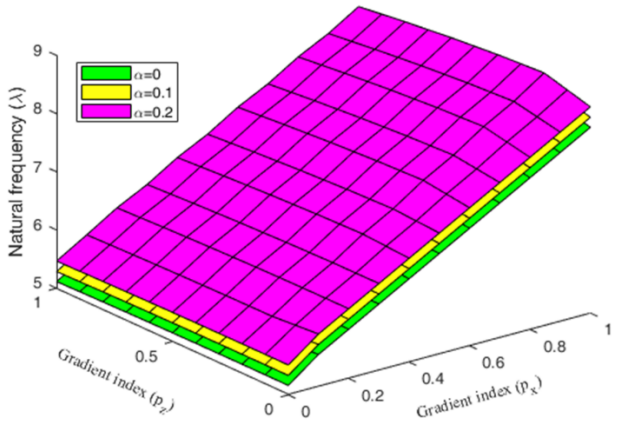

Fig. 8. Effect of α on λ for CC 2D-FGPB with un-even porosity at aspect ratio L/h=5

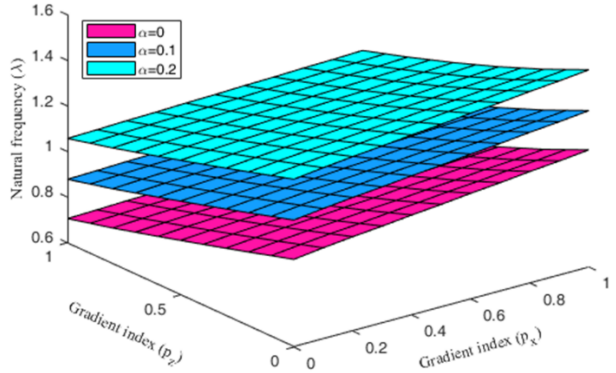

Fig. 9. Effect of α on λ for CF 2D-FGPB with even porosity at aspect ratio L/h=5

As the porosity index (α) grows, from Figs. 5 - 10, it is possible to detect that the disparity that exists between the various patterns of porosity distribution can become even more pronounced. On the other hand, free vibration occurs more frequently in regions with an even porosity distribution as compared to regions with an uneven porosity distribution [28].

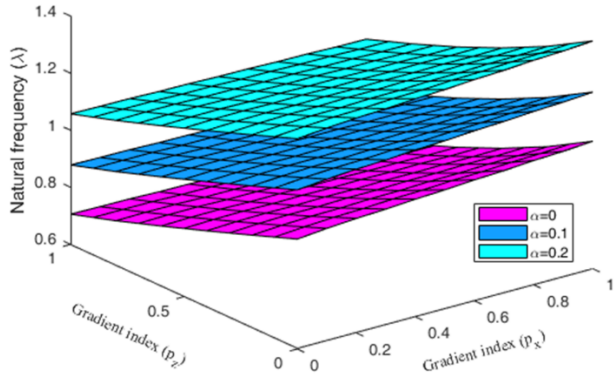

Fig. 10. Effect of α on λ for CF 2D-FGPB with un-even porosity at aspect ratio L/h=5

The free vibration value of an SS beam falls when the gradation exponents in the *x* as well as *z* directions are increased and rises when the porosity index is increased. If there is an even distribution of porosity across the material, the vibration value will be higher than if there is an uneven distribution. It should be observed that the free vibration proves to be increasing with the porosity coefficient, and that the influence of this increase is more significant at a high porosity value [32]. This is because there is a decrease in flexible stiffness when the porosity value is increased. Additionally, it has been shown that the vibration lessens when there is an increase in the gradient index; this holds true for both the even as well as uneven porosity. The beam is considered to be pure metal and has a lower stiffness when the gradient index is equal to zero (p = 0). As the gradient index (p) approaches infinity, a beam approaches the characteristics of a pure ceramic with a high stiffness, which results in decreased vibration [23].

4. Conclusion

Under various boundary circumstances, two- directional FG porous beams were studied for free vibration (SS, CC, and CF). These boundary conditions had various aspect ratios and gradation exponents on the x and z axes. The n^{th} order shear deformation theory was adapted to calculate free vibration for FG porous beams with both even as well as uneven porosity.

The properties that determine the behavior of 2D-FGPB were calculated using a power law distribution. The computed dimensionless free vibrations are compared with published research and are in good agreement. Findings of the vibration analysis are summarised and listed below:

- The dimensionless natural frequency decreases during the transition from the CC boundary condition to the SS and CF boundary conditions. This suggests a decrease in the beam's stiffness and rigidity as the boundary conditions become less restrictive.
- The dimensionless free vibration of 2D-FGPB is strongly affected by gradient indices. But the gradient index affects *x* to a greater extent than *z*.
- As the volume percentage of porosity around the centre surface increases, free vibration will also increase.
- Shear deformation affects 2D-FGPB vibration as aspect ratio increases. The CC 2D-FGPB is more vulnerable to shear deformation than other models.
- Shear deformation has a significant effect, particularly for thick beams, and the proposed theory accurately predicts and explains the vibration patterns of 2D-FGPB.
- The gradient indices and the selection of boundary conditions exert a substantial impact on the dimensionless natural frequency of the 2D-FGPB. Variations in the beam's stiffness and subsequent effects on its vibration characteristics are influenced by different values of the gradient indices and boundary conditions.

The research findings hold several practical implications for both materials engineering and structural design. The significant influence of boundary conditions and gradient indices on the natural frequency of 2D-FGPBs can be leveraged to make informed decisions about material and selection and structural design. This understanding could be valuable for applications requiring vibration control, enabling the design of 2D-FGPBs with specific properties to effectively mitigate vibrations. The porosity parameter is an important factor that must be taken into account when designing contemporary structures, as the amount of porosity in a structure can significantly impact its performance and response. The proposed theory may not accurately predict the behaviour of structures with large deflections or large deformations, as it is based on linear elasticity assumptions. The proposed method can be used to analyze 2D-FGPB surfaces that are exposed to high temperatures at one end and low temperatures at the other in further studies. Future work could involve experimental validation, optimization algorithms for tailored material properties, dynamic analysis, and the exploration of advanced materials and their real-world applications. Evaluating the environmental impact of 2D-FGPBs could also be a relevant focus, aligning with the growing emphasis on sustainability in engineering practices.

References

[1] Y. Miyamoto, W.A. Kaysser, B.H. Rabin, A. Kawasaki, and R.G. Ford, R.G, *Processing and fabrication. In Functionally Graded Materials*. Bostom: Springer, 1999.

[2] S. R. Asemi, A. Farajpour, H. R. Asemi, and M. Mohammadi, "Influence of initial stress on the vibration of double-piezoelectric-nanoplate systems with various boundary conditions using DQM", *Physica E*, vol. 63, pp. 169-179, Sep. 2014, doi: 10.1016/j.physe.2014.05.009.

[3] N. Hebbar, I. Hebbar, D. Ouinas, and M. Bourada, "Numerical modeling of bending, buckling, and vibration of functionally graded beams by using a higher-order shear deformation theory", *Frat. ed Integrità Strutt*, vol. 14, no. 52, pp. 230-246, Mar. 2020, doi: 10.3221/IGF-ESIS.52.18.

[4] A. Farajpour, A. Rastgoo, and M. Mohammadi, "Surface effects on the mechanical characteristics of microtubule networks in living cells", *Mech. Res. Commun*., vol. 57, pp. 18-26, Apr. 2014, doi: 10.1016/j.mechrescom.2014.01.005.

[5] M. Mohammadi, M. Safarabadi, A. Rastgoo, and A. Farajpour, "Hygro-mechanical vibration analysis of a rotating viscoelastic nanobeam embedded in a visco-Pasternak elastic medium and in a nonlinear thermal environment", *Acta Mech*., vol. 227, no. 8, pp. 2207-2232, 2016, doi: 10.1007/s00707-016-1623-4.

[6] H. Bellifa, K.H. Benrahou, L. Hadji, M.S.A. Houari, and A. Tounsi, "Bending and free vibration analysis of functionally graded plates using a simple shear deformation theory and the concept the neutral surface position", *J. Braz. Soc. Mech. Sci. Eng*., vol. 38, no. 1, pp. 265-275, Jan. 2016, doi: 10.1007/s40430-015-0354-0.

[7] T.K. Nguyen, T.T.P. Nguyen, T.P. Vo, and H.T. Thai, "Vibration and buckling analysis of functionally graded sandwich beams by a new higher-order shear deformation theory", *Composites, Part B*, vol. 76, pp. 273-285, Jul. 2015, doi: 10.1016/j.compositesb.2015.02.032.

[8] A.S. Sayyad, and Y.M. Ghugal, "A unified shear deformation theory for the bending of isotropic, functionally graded, laminated and sandwich beams and plates", *Int. J. Appl. Mech*., vol. 9, no. 1, 1750007, Jan. 2017, doi: 10.1142/S1758825117500077.

[9] Z. F. Zohra, H.H. Lemya, Y. Abderahman, M. Mustapha, T. Abdelouahed, and O. Djamel, "Free vibration analysis of functionally graded beams using a higher-order shear deformation theory", *Math. Model. Eng*., vol. 4, no. 1, pp. 7-12, Mar. 2017, doi: 10.18280/mmep.040102.

[10] A.S. Sayyad, and Y.M. Ghugal, "Bending buckling and free vibration responses of hyperbolic shear deformable FGM beams", *Mech. Adv. Compos. Struct*., vol. 5, no. 1, pp. 13-24, Apr. 2018, doi: 10.22075/MACS.2018.12214.1117.

[11] T. Van Do, D.K. Nguyen, N.D. Duc, D.H. Doan, and T.Q. Bui, "Analysis of bi-directional functionally graded plates by FEM and a new third-order shear deformation plate theory", *Thin-Walled Struct*., vol. 119, pp. 687-699, Oct. 2017, doi: 10.1016/j.tws.2017.07.022

[12] S. Coskun, J. Kim, and H. Toutanji, "Bending, free vibration, and buckling analysis of functionally graded porous micro-plates using a general third-order plate theory", *J. Compos. Sci.*, vol. 3, no. 1, pp. 2-22, Feb. 2019, doi: 10.3390/jcs3010015.

[13] A. Mojahedin, M. Jabbari, and T. Rabczuk, "Thermoelastic analysis of functionally graded porous beam", *J. Therm. Stresses*, vol. 41, no. 8, pp. 937-950, Aug. 2018, doi: 10.1080/01495739.2018.1446374.

[14] M. Babaei, K. Asemi, and P. Safarpour, "Natural frequency and dynamic analyses of functionally graded saturated porous beam resting on viscoelastic foundation based on higher order beam theory", *J. Solid Mech*., vol. 11, no. 3, pp. 615-634, Sep. 2019, doi: 10.22034/JSM.2019.666691.

[15] T.Q. Hung, D.M. Duc, and T.M. Tu, "Static Behavior of Functionally Graded Sandwich Beam with Fluid-Infiltrated Porous Core", *In Modern Mechanics and Applications: Select Proceedings of ICOMMA*, Singapore, 2022, pp. 691-706.

[16] M. Gharibi M. Zamani Nejad, and A. Hadi, "Elastic analysis of functionally graded rotating thick cylindrical pressure vessels with exponentially-varying properties using power series method of Frobenius", *J. Comput. Appl. Mech*., vol. 48, no. 1, pp. 89-98, Jun. 2017, doi: 10.22059/jcamech.2017.233633.143.

[17] H.Q. Tran, V.T. Vu, and M.T. Tran, "Free vibration analysis of piezoelectric functionally graded porous plates with graphene platelets reinforcement by pb-2 Ritz method", *Compos. Struct.*, vol. 305, 116535, Feb. 2023, doi: 10.1016/j.compstruct.2022.116535.

[18] P. Van Vinh, M. Avcar, and M.O. Belarbi, A. Tounsi, "A new higher-order mixed four-node quadrilateral finite element for static bending analysis of functionally graded plates", *Struct*., vol. 47, pp. 1595-1612, Jan. 2023, doi: 10.1016/j.istruc.2022.11.113.

[19] B. Karami, D. Shahsavari, M. Janghorban, and L. Li, "On the resonance of functionally graded nanoplates using bi-Helmholtz

nonlocal strain gradient theory", *Int. J. Eng. Sci*., vol. 144, 103143, Nov. 2019, doi: 10.1016/j.ijengsci.2019.103143.

[20] E. Zarezadeh, V. Hosseini, and A. Hadi, "Torsional vibration of functionally graded nano-rod under magnetic field supported by a generalized torsional foundation based on nonlocal elasticity theory", *Mech. Based Des. Struct. Mach*., vol. 48, no. 4, pp. 480-495, Jul. 2020, doi: 10.1080/15397734.2019.1642766.

[21] Y. Tang, and Q. Ding, "Nonlinear vibration analysis of a bi-directional functionally graded beam under hygro-thermal loads", Compos. Struct., vol. 225, 111076, Oct. 2019, doi: 10.1016/j.compstruct.2019.111076.

[22] M. Şimşek, "Buckling of Timoshenko beams composed of two-dimensional functionally graded material (2D-FGM) having different boundary conditions", *Compos. Struct*., vol. 149, pp. 304-314, Aug. 2016, doi: 10.1016/j.compstruct.2016.04.034.

[23] A. Karamanli, "Free vibration analysis of two directional functionally graded beams using a third order shear deformation theory", *Compos. Struct*., vol. 189, pp. 127-136, Apr. 2018, doi: 10.1016/j.compstruct.2018.01.060.

[24] T. Van Do, D.K. Nguyen, N.D. Duc, D.H. Doan, and T.Q. Bui, "Analysis of bi-directional functionally graded plates by FEM and a new third-order shear deformation plate theory", *Thin-Walled Struct*., vol. 119, pp. 687-99, Oct. 2017, doi: 10.1016/j.tws.2017.07.022.

[25] A.M. Zenkour, "Quasi-3D refined theory for functionally graded porous plates: displacements and stresses", *Phys. Mesomech*., vol. 23, no. 1, pp. 39-53, Jan. 2020, doi: 10.1134/S1029959920010051.

[26] M. Kaddari, A. Kaci, A.A. Bousahla, A. Tounsi, F. Bourada, E.A. Bedia, M.A. and Al-Osta, "A study on the structural behaviour of functionally graded porous plates on elastic foundation using a new quasi-3D model: Bending and free vibration analysis, *Comput. Concr*., vol. 25, no. 1, pp. 37-57, Jan. 2020, doi: 10.12989/cac.2020.25.1.037.

[27] S. Zghal, S. Ataoui, and F. Dammak, "Static bending analysis of beams made of functionally graded porous materials", *Mech. Based Des. Struct. Mach*., vol. 50, no. 3, pp. 1012-1029, Mar. 2022, doi: 10.1080/15397734.2020.1748053.

[28] G. Reddy, and N.V. Kumar, "Free Vibration Analysis of 2D Functionally Graded Porous Beams Using Novel Higher-Order Theory", *Mech. Adv. Compos. Struct*., vol. 10, no. 1, pp. 69-84, Apr. 2023, doi: 10.22075/MACS.2022.28118.1428.

[29] V.K. Nathi, "Buckling analysis of 2D functionally graded porous beams using novel higher order theory", *J. Comput. Appl. Mech*., vol. 53, no. 3, pp. 393-413, Sep. 2022, doi: 10.22059/jcamech.2022.345384.736.

[30] T.P. Vo, H.T. Thai, T.K. Nguyen, and F. Inam, "Static and vibration analysis of functionally graded beams using refined shear deformation theory", *Meccanica*, vol. 49, no. 1, pp. 155-168, Jan. 2014, doi: 10.1007/s11012-013-9780-1.

[31] A. Karamanlı, "Bending behaviour of two directional functionally graded sandwich beams by using a quasi-3d shear deformation theory", *Compos. Struct*., vol. 174, pp. 70-86, Aug. 2017, doi: 10.1016/j.compstruct.2017.04.046.

[32] M.R. Galeban, A. Mojahedin, Y. Taghavi, and M. Jabbari, "Free vibration of functionally graded thin beams made of saturated porous materials", *Steel and Compos. Struct*., vol. 21, no. 5, pp. 999-1016, Jul. 2016, doi: 10.12989/scs.2016.21.5.999.

[33] G. Reddy, and N.V. Kumar, "Bending Analysis of 2-D Functionally Graded Porous Beams Based on Novel High Order Theory", *J. Eng. Sci. Technol. Rev*., vol. 15, no. 5, Aug. 2022, doi: 10.25103/jestr.155.24.

[34] V.I. Rizov, "Analyses of Delamination in Functionally Graded Multilayered Beams", *J. Eng. Sci. Technol. Rev*., vol. 10, no. 6, pp. 111-118, Nov. 2017, doi: 10.25103/jestr.106.15.

[35] P. Bridjesh, N.K. Geetha, and B. Yelamasetti, "Numerical investigation on buckling of two-directional porous functionally graded beam using higher order shear deformation theory", *Int. J. Interact. Des. Manuf.,* pp. 1-14, May. 2023, doi: 10.1007/s12008-023-01332-6.

Nomenclature

2D-FGPB	Two- directional functionally graded porous beam
CBT	Classical beam theory
CC	Clamped-clamped
CF	Clamped free
E	Modulus of elasticity (GPa)
FG	Functionally graded
FGB	Functionally graded beam
FGM	Functionally graded material
f(z)	Shear shape function
h	Height (m)
HSDT	Higher order shear deformation theory
K	Shear correction factor
L	Length (m)
UDL	Uniformly distributed load
p_x	Gradient index in the length direction
p_z	Gradient index in the thickness direction
SS	Simply supported
V_f	Volume fraction
x, y, z	Different coordinates along length, width, and thickness directions of beam
α	Coefficient of porosity/ Porosity index
μ	Poisson's ratio
ρ	Mass density (Kg/m^3)
δU	Strain energy
δk	Kinetic energy
ϕ	Shear slope
$\frac{\partial w_0}{\partial x}$	Bending slope